Rates of Platination of AG and GA Containing Double-Stranded Oligonucleotides: Insights into Why Cisplatin Binds to GG and AG but Not GA Sequences in DNA

Murray S. Davies,[†,‡] Susan J. Berners-Price,*[,†] and Trevor W. Hambley*[,‡]

Contribution from the School of Science, Griffith University, Nathan, Brisbane, QLD 4111, Australia, and School of Chemistry, University of Sydney, Sydney, NSW 2006, Australia

Received May 18, 1998

Abstract: The reactions of the self-complementary 14-base-pair duplexes 5′-d(AATT**AG**TACTAATT)-3′ (-**AG**-) and 5′-d(AATT**GA**TATCAATT)-3′ (-**GA**-) with ^{15}N-cisplatin, (*cis*-[PtCl$_2$(^{15}NH$_3$)$_2$]) (pH 6.0, T = 298 K) and *cis*-[Pt(^{15}NH$_3$)$_2$(OH$_2$)$_2$]$^{2+}$ (pH 4.9, T = 288 K), have been investigated using [^{1}H,^{15}N] HSQC 2D NMR spectroscopy. Reactions involving cisplatin progress via the hydrolysis product *cis*-[PtCl(NH$_3$)$_2$(OH$_2$)]$^+$. Two major -**AG**- monofunctional adducts, G(6)/Cl and A(5)/Cl, form at rates of 1.06 ± 0.06 and 0.149 ± 0.014 M^{-1} s^{-1}, respectively. The major Pt-**GA**- monofunctional adduct G(5)/Cl forms at a rate of 0.023 ± 0.002 M^{-1} s^{-1}, and several minor adducts, including A(6)/Cl (0.0054 ± 0.0010 M^{-1} s^{-1}), are observed. Closure from the monofunctional/Cl adducts proceeds via an aquated species for both -**AG**- and -**GA**-. The rates of hydrolysis from the G/Cl adducts to the G/H$_2$O species are (1.55 ± 0.05) × 10^{-5} s^{-1} with -**AG**- and (0.198 ± 0.008) × 10^{-5} s^{-1} with -**GA**-, and the rates of closure to the chelates are (9.8 ± 0.9) × 10^{-5} and (0.69 ± 0.17) × 10^{-5} s^{-1} for -**AG**- and -**GA**-, respectively. The rates of ring closure from A/Cl monofunctional species, treated as direct to chelate, are (0.16 ± 0.06) × 10^{-5} (-**AG**-) and (2.1 ± 0.7) × 10^{-5} s^{-1} (-**GA**-). The rate constants found for the reactions between the oligonucleotides and *cis*-[Pt(^{15}NH$_3$)$_2$(OH$_2$)$_2$]$^{2+}$ are, for formation of the G/H$_2$O monofunctional adducts, 0.42 ± 0.01 (-**AG**-) and 0.50 ± 0.01 M^{-1} s^{-1} (-**GA**-). Formation of A/H$_2$O adducts is not observed for either -**AG**- or -**GA**-. Rates of ring closure from the G/H$_2$O adducts are (3.71 ± 0.05) × 10^{-5} (-**AG**-) and (0.162 ± 0.005) × 10^{-5} s^{-1} (-**GA**-). The rate of formation of monofunctional adducts from *cis*-[Pt(^{15}NH$_3$)$_2$(OH$_2$)$_2$]$^{2+}$ are similar for -**AG**- and -**GA**-, whereas for cisplatin a clear preference is observed for -**AG**- over -**GA**-. Closure to form the bifunctional adduct is more rapid in the case of -**AG**- than -**GA**- for both cisplatin and *cis*-[Pt(^{15}NH$_3$)$_2$(OH$_2$)$_2$]$^{2+}$, but the difference is greater for *cis*-[Pt(^{15}NH$_3$)$_2$(OH$_2$)$_2$]$^{2+}$. It is concluded that the bifunctional intrastrand adduct profile observed when cisplatin binds to DNA is substantially controlled by the rate of formation of monofunctional adducts at the different X-purine-purine-X sequences. A slow rate of closure also contributes to the nonformation of the bifunctional GpA adduct.

Introduction

When the anticancer agent cisplatin, *cis*-[PtCl$_2$(NH$_3$)$_2$] (**1**), binds to DNA, the major adducts are GG and AG intrastrand cross-links that account for about 65% and 25%, respectively, of the bound Pt in vitro.[1−6] Similar results are found for *cis*-[PtCl$_2$(en)] (en = 1,2-diaminoethane)[2,7] and the *R*,*R*- and *S*,*S*-enantiomers of *cis*-[PtCl$_2$(1,2-dach)], (dach = 1,2-diaminocyclohexane),[8] while decreases in GG (54%) and AG (8%) and an increase in GpNpG (18%) were found with *cis*-[PtCl$_2$(NH$_3$)(NH$_2$C$_6$H$_{11}$)], a metabolite of the orally administrable *cis,trans,-cis*-[PtCl$_2$(O$_2$CC$_3$H$_7$)$_2$(NH$_3$)(NH$_2$C$_6$H$_{11}$)].[9] No bifunctional binding to GA sequences is observed for any of these compounds, although Leng and co-workers[4] have provided some evidence for binding to GpA in a sequence lacking a GpG site, and Murray et al.[10,11] have observed Pt binding at GpA sites but could not determine whether it was bifunctional. Pt is known to have a strong kinetic preference for binding to guanine over adenine[12−17] and this may contribute to the preference for

* To whom correspondence should be addressed. (T.W.H.) Phone: 61-2-9351-2830. Fax: 61-2-9351-3329. E-mail: t.hambley@chem.usyd.edu.au. (S.J.B.-P.) E-mail: S.Berners-Price@sct.gu.edu.au.

† Griffith University.

‡ University of Sydney.

(1) Eastman, A. *Biochemistry* **1982**, *21*, 6732−6736.
(2) Eastman, A. *Biochemistry* **1983**, *22*, 3927−3933.
(3) Fichtinger-Schepman, A.-M. J.; van der Veer, J. L.; den Hartog, J. H. J.; Lohman, P. H. M.; Reedijk, J. *Biochemistry* **1985**, *24*, 707−713.
(4) Decoville, M.; Schwartz, A.; Locker, D.; Leng, M. *FEBS Lett.* **1993**, *323*, 55−58.
(5) Eastman, A. *Pharmac. Ther.* **1987**, *34*, 155−166.
(6) Lippard, S. J. *Pure Appl. Chem.* **1987**, *59*, 731−742.
(7) Eastman, A. *Biochemistry* **1986**, *25*, 3912−3915.
(8) Jennerwein, M. M.; Eastman, A.; Khokhar, A. *Chem. Biol. Int.* **1989**, *70*, 39−49.
(9) Hartwig, J. F.; Lippard, S. J. *J. Am. Chem. Soc.* **1992**, *114*, 5646−5654.
(10) Murray, V.; Motyka, H.; England, P. R.; Wickham, G.; Lee, H. H.; Denny, W. A.; McFadyen, W. D. *Biochemistry* **1992**, *31*, 11812−11817.
(11) Murray, V.; Motyka, H.; England, P. R.; Wickham, G.; Lee, H. H.; Denny, W. A.; McFadyen, W. D. *J. Biol. Chem.* **1992**, *267*, 18805−18808.
(12) Martin, R. B. *Acc. Chem. Res.* **1985**, *18*, 32−38.
(13) Bancroft, D. P.; Lepre, C. A.; Lippard, S. J. *J. Am. Chem. Soc.* **1990**, *112*, 6860−6871.
(14) Eapen, S.; Green, M.; Ismail, I. M. *J. Inorg. Biochem.* **1985**, *24*, 233−237.
(15) Arpalahti, J.; Lippert, B. *Inorg. Chem.* **1990**, *29*, 104−110.
(16) Mansy, S.; Chu, G. Y. H.; Duncan, R. E.; Tobias, R. S. *J. Am. Chem. Soc.* **1978**, *100*, 607−616.

10.1021/ja981725u CCC: $15.00
Published on Web 10/27/1998

binding to GG over AG but it cannot be the sole cause of the nonformation of bifunctional GA adducts.

Pt does bind bifunctionally to the dinucleotide d(GpA),[18,19] and therefore the structure of duplex DNA must contribute substantially to its nonformation thereon. Two explanations have been put forward for this. Dewan[20] suggested that, when Pt is bound to the G of an AGA sequence on B-DNA, the distance to the 5′-A (∼3 Å) is less than the distance to the 3′-A (∼5 Å) and has proposed that this leads to a preference for Pt-AG chelate formation over Pt-GA chelate formation. One of us has pointed out that this depends on how these distances are measured[21,22] and that the distances change substantially if the DNA conformation changes. It was suggested, instead, that the destabilization of the GA adduct may be due to repulsive interactions between one of the NH_3 ligands and the exocyclic NH_2 group of the adenine.[21,22] A detailed understanding of why cisplatin binds to GG in preference to AG and why GA adducts are not observed at all should improve our understanding of the factors that control Pt/DNA interactions and assist in the rational development of agents that target sequences different from those favored by cisplatin.

Pt binding to DNA is kinetically controlled, and there have been a number of recent studies where the rate of binding to the different nucleotide bases has been examined.[13,15−17] Bancroft et al.[13] used ^{195}Pt NMR to determine the rates of the reactions of cisplatin and *trans*-$[PtCl_2(NH_3)_2]$ with chicken erythrocyte DNA. They found that both formation of monofunctional adducts and closure to bifunctional adducts were pseudo-first-order processes and in the case of cisplatin the rates were similar at $(10.2 \pm 0.7) \times 10^{-5}$ and $(9.2 \pm 1.4) \times 10^{-5}$ s^{-1}. Chottard and colleagues[23,24] have recently determined the rates of the reactions between *cis*-$[Pt(NH_3)_2(OH_2)_2]^{2+}$ (**2**) and short single- and double-stranded oligonucleotides containing GG sequences by trapping the intermediates, separating them quantitatively using HPLC, and isolating the platinated sites by enzymatic digestion. In this way, they were able to identify the two monofunctional adducts (5′ and 3′) and detect significant differences in their rates of formation and rates of closure to the bifunctional adduct.

Similar results have been obtained by Sadler and colleagues[25−27] using [^{1}H,^{15}N] HSQC (heteronuclear single-quantum coherence) 2D NMR spectroscopy to monitor the reaction between ^{15}N-labeled cisplatin or *cis*-$[Pt(^{15}NH_3)_2(OH_2)_2]^{2+}$ and a 14-base-pair duplex with a GG binding site. This approach is particularly attractive because spectra can be acquired quickly (in as little as 3−4 min), all platinated species are observed at micromolar concentrations, and spectra are simplified because only the shifts of the two platinum-bound ammine ^{1}H and ^{15}N nuclei are seen, and these are highly sensitive to the nature of the ligand trans to them.[28−30]

Therefore, we have used [^{1}H,^{15}N] HSQC 2D NMR spectroscopy to investigate the kinetics of the reactions between ^{15}N-labeled cisplatin and its fully aquated analogue *cis*-$[Pt(^{15}NH_3)_2(OH_2)_2]^{2+}$, with two 14-base-pair self-complementary oligonucleotides: 5′-d(AATT**AG**TACTAATT)-3′ containing a 5′-AG-3′ grouping and 5′-d(AATT**GA**TATCAATT)-3′ containing a 5′-GA-3′ site, where the bold lettering indicates the expected sites of platination.

Experimental Section

Chemicals. *cis*-$[PtCl_2(^{15}NH_3)_2]$ was synthesized according to Kerrison and Sadler[31] and recrystallized from aqueous KCl. The sodium salts of HPLC-purified oligonucleotides were purchased from OSWEL.

Sample Preparation. A stock solution (6.037 mM) of *cis*-$[Pt(^{15}NH_3)_2(OH_2)_2](ClO_4)_2$ was prepared by treatment away from light of *cis*-$[PtCl_2(^{15}NH_3)_2]$ (19.98 mg, 6.62×10^{-5} mol) with $AgNO_3$ (22.12 mg, 1.30×10^{-4} mol, 1.97 equiv) in dimethylformamide (DMF)-d_7 (204 μL).[32] The suspension was sonicated at 310 K for 15 min and then incubated at that temperature for 24 h. The solution was centrifuged and 52.7 μL of the supernatant solution removed with a micropipet. This was diluted with 2.78 mL of 0.1 M $NaClO_4$ in 10% D_2O in H_2O. The [^{1}H,^{15}N] HSQC 2D NMR spectrum showed this to be pure *cis*-$[Pt(^{15}NH_3)_2(OH_2)_2]^{2+}$ with no cisplatin or *cis*-$[PtCl(^{15}NH_3)_2(OH_2)]^+$.

Stock Solutions of Oligonucleotides. The $Na^+/O_2CCH_3^-$ salts of 5′-d(AATT**GA**TATCAATT)-3′ (-**GA**-) (3.8063 μmol) and 5′-d(AATT-**AG**TACTAATT)-3′ (-**AG**-) (3.5357 μmol) were each dissolved in 10% D_2O in H_2O (220 μL).

Reaction of Duplex -AG- with ^{15}N-Cisplatin. -**AG**- stock solution (110 μL, 8.84×10^{-7} mol of duplex), sodium phosphate solution (19.4 μL, 200 mM, pH 6.0), TSP (sodium 3-trimethylsilyl-$_{D4}$-propionate) (1.2 μL of 13.3 mM), and 10% D_2O in H_2O (258 μL) were combined, and the pH was measured (pH = 6.1). A 40-μL aliquot of freshly prepared *cis*-$[PtCl_2(^{15}NH_3)_2]$ (3.25 mg, 10.8 μmol) in 10% D_2O in H_2O (1000 μL) was added, giving concentrations of -**AG**- duplex, 1.89 mM, sodium phosphate, 9.0 mM, and *cis*-$[PtCl_2(^{15}NH_3)_2]$, 1.84 mM.

Reaction of Duplex -GA- with ^{15}N-Cisplatin. -**GA**- stock solution (110 μL, 9.52×10^{-7} mol of duplex), sodium phosphate solution (27.1 μL, 200 mM, pH 6.0), TSP (2.0 μL of 13.3 mM), and 10% D_2O in H_2O (353 μL) were combined, and the pH was determined (pH = 6.0). To this solution was added a 108-μL aliquot of freshly prepared *cis*-$[PtCl_2(^{15}NH_3)_2]$ (2.4 mg, 7.9 μmol) in 10% D_2O in H_2O (1000 μL), giving final concentrations of -**GA**- duplex, 1.59 mM, sodium phosphate, 9.0 mM, and *cis*-$[PtCl_2(^{15}NH_3)_2]$, 1.43 mM.

Reaction of Duplex -AG- with *cis*-$[Pt(^{15}NH_3)_2(OH_2)_2]^{2+}$. -**AG**- stock solution (110 μL, 8.84×10^{-7} mol of duplex), $NaClO_4$ (46 μL, 1.0 M), and 10% D_2O in H_2O (224 μL) were combined. The pH was measured (pH = 6.0) and adjusted to 4.9 with HNO_3 (12 μL of 1.0 M). A total of 30 μL of the solution was removed for pH measurement. To the remaining solution was added a 100-μL aliquot of the 6.037 mM stock solution of *cis*-$[Pt(^{15}NH_3)_2(OH_2)_2]^{2+}$ (pH 4.3) to give final concentrations of -**AG**- duplex, 1.69 mM, ClO_4^-, 0.1 M, and *cis*-$[Pt(^{15}NH_3)_2(OH_2)_2]^{2+}$, 1.27 mM.

Reaction of Duplex -GA- with *cis*-$[Pt(^{15}NH_3)_2(OH_2)_2]^{2+}$. -**GA**- stock solution (110 μL, 9.52×10^{-7} mol of duplex), $NaClO_4$ (62 μL, 1.0 M), and 10% D_2O in H_2O (434.5 μL) were combined. The pH

(17) Marcelis, A. T. M.; Erkelens, C.; Reedijk, J. *Inorg. Chim. Acta* **1984**, *91*, 129−135.
(18) Dijt, F. J.; Chottard, J.-C.; Girault, J.-P.; Reedijk, J. *Eur. J. Biochem.* **1989**, *179*, 333−344.
(19) Hemelryck, J.; Girault, J.-P.; Chottard, G.; Valadon, P.; Laoui, A.; Chottard, J.-C. *Inorg. Chem.* **1987**, *26*, 787−795.
(20) Dewan, J. C. *J. Am. Chem. Soc.* **1984**, *106*, 7239−7244.
(21) Hambley, T. W. *J. Chem. Soc., Chem. Commun.* **1988**, 221−223.
(22) Hambley, T. W. *Inorg. Chem.* **1991**, *30*, 937−942.
(23) Gonnet, F.; Reeder, F.; Kozelka, J.; Chottard, J.-C. *Inorg. Chem.* **1996**, *35*, 1653−1658.
(24) Reeder, F.; Gonnet, F.; Kozelka, J.; Chottard, J.-C. *Chem. Eur. J.* **1996**, *2*, 1068−1076.
(25) Barnham, K. J.; Berners-Price, S. J.; Frenkiel, T. A.; Frey, U.; Sadler, P. J. *Angew. Chem., Int. Ed. Engl.* **1995**, *34*, 1874−1877.
(26) Berners-Price, S. J.; Barnham, K. J.; Frey, U.; Sadler, P. J. *Chem. Eur. J.* **1996**, *2*, 1283−1291.
(27) Reeder, F.; Guo, Z.; Murdoch, P. del S.; Corazza, A.; Hambley, T. W.; Berners-Price, S. J.; Chottard, J.-C.; Sadler, P. J. *Eur. J. Biochem.* **1997**, *249*, 370−382.
(28) Barnham, K. J.; Berners-Price, S. J.; Guo, Z.;. Murdoch, P. del S.; Sadler, P. J. NMR spectroscopy of platinum drugs: from DNA to body fluids. In Pinedo, H. M., Schornagel, J. H., Eds.; Platinum and other metal coordination compounds in cancer chemotherapy 2; Plenum Press: New York, 1996; pp 1−16.
(29) Berners-Price, S. J.; Sadler, P. J. *Coord. Chem. Rev.* **1996**, *151*, 1−40.
(30) Appleton, T. G.; Hall, J. R.; Ralph, S. F. *Inorg. Chem.* **1985**, *24*, 4685−4693.
(31) Kerrison, S. J. S.; Sadler, P. J. *J. Chem. Soc., Chem. Commun.* **1977**, 861−864.
(32) Berners-Price, S. J.; Frey, U.; Ranford, J. D.; Sadler, P. J. *J. Am. Chem. Soc.* **1993**, *115*, 8649−8659.

was measured (pH = 6.0) and adjusted to 4.9 with HNO_3 (11.6 μL of 1.0 M in 10% D_2O in H_2O), 30 μL of the solution was removed for pH measurement, and to the remaining solution was added a 108-μL aliquot of the 6.037 mM stock *cis*-$[Pt(^{15}NH_3)_2(OH_2)_2]^{2+}$ solution (pH 4.3). The final concentrations were -**GA**- duplex, 1.30 mM, ClO_4^-, 0.10 M, and *cis*-$[Pt(^{15}NH_3)_2(OH_2)_2]^{2+}$, 0.94 mM.

Instrumentation. The 599.924-MHz $^1H\{^{15}N\}$ NMR spectra were recorded on a Varian UNITY-INOVA 600-MHz spectrometer fitted with a pulsed gradient module and a 5-mm inverse probehead. The ^1H spectra were acquired with water suppression using the WATERGATE sequence.[33] Both the 1D ^{15}N-edited ^1H NMR spectra and 2D [^1H,^{15}N] HSQC NMR spectra (optimized for $^1J(^{15}N,^1H) = 72$ Hz) were recorded using the sequence of Stonehouse et al.[34] In this sequence, suppression of the H_2O signal and coherence selection are achieved using gradient pulses, and H_2O magnetization is returned to its equilibrium position (*z* axis) prior to the start of data acquisition. Samples were not spun during the acquisition of data. All samples (including buffers, acids, etc.) were prepared so that there was a 90% H_2O/10% D_2O concentration (for deuterium lock but with minimal loss of signal as a result of deuterium exchange).

^1H chemical shifts were referenced to internal TSP (for cisplatin reactions); those in *cis*-$[Pt(^{15}NH_3)_2(OH_2)_2]^{2+}$ reactions were calibrated using the ^1H resonance at 2.0 ppm at pH 4.9 of the acetate impurity in the oligonucleotide sample. ^{15}N chemical shifts were calibrated externally against $^{15}NH_4Cl$ (1.0 M in 1.0 M HCl in 5% D_2O in H_2O).[26] The ^{15}N signals were decoupled by irradiating with the GARP-1 sequence at a field strength of 1 kHz during the acquisition time.

Typically for 1D ^1H spectra, 64 or 128 transients were acquired using a spectral width of 12 kHz, a relaxation delay of 1.5 s, and a line broadening of 1.0 Hz. For kinetics studies involving [^{15}N,^1H] HSQC spectra, between 4 and 12 transients were collected for 16−64 increments of t_1 (allowing spectra to be recorded on a suitable time scale for the observed reaction), with an acquisition time of 0.152 s and spectral widths of 4 kHz in f_2 (^1H) and 2 kHz in f_1 (^{15}N). 2D spectra were completed in 4−60 min.

The 2D spectra were processed using Gaussian weighting functions in both dimensions and zero-filling by ×2 in the f_1 dimension. The pH of the solutions was measured on a Shindengen pH Boy-P2(su19A) pH meter and calibrated against pH buffers at pH 6.9 and 4.0. A volume of 10 μL of the solution was placed on the electrode surface and the pH recorded. These aliquots were not returned to the bulk solution (as the electrode leaches Cl^-). Adjustments in pH were made using 1.0 M HNO_3 in 10% D_2O in H_2O, or 1.0 M NaOH in 10% D_2O in H_2O.

Cisplatin reactions were carried out in buffered (sodium phosphate, 9 mM, pH 6.0) solution at 298 K, while the *cis*-$[Pt(^{15}NH_3)_2(OH_2)_2]^{2+}$ reactions were at pH 4.9, unbuffered in 0.1 M $NaClO_4$ at 288 K. At this pH, the aqua ligands are neutral ($pK_{a1} = 5.37$, $pK_{a2} = 7.21$)[35] and the N7 of guanine is deprotonated. The duplex structure is stable at this pH, although a pH-induced structural change for a similar duplex containing a GG site is observed at pH 4.7, brought about by protonation of cytosine.[36] The solutions were maintained at these temperatures when not immersed in the NMR probe.

Data Analysis. The kinetic analysis of the reactions was undertaken by measuring the peak volumes in the [^1H,^{15}N] HSQC 2D spectra using the Varian VNMR software and calculating relative concentrations of *cis*-$\{Pt(^{15}NH_3)_2\}$ at each time point. For a given reaction, peak volumes were determined using an identical vertical scale and threshold value. It is assumed that all peaks have ^{195}Pt satellites; only those of cisplatin are visible in the spectra, and their absence in other species is presumably a consequence of relaxation through chemical shift anisotropy.[37] All species, other than cisplatin and *cis*-$[Pt(^{15}NH_3)_2(OH_2)_2]^{2+}$, give rise to two peaks, the inequivalence of the NH_3 groups being due to the ligands trans to them. In some cases, overlap between peaks is significant, but in these instances, it was only one of the pair of the peaks that was overlapped. Thus, reliable intensities were obtained from the second of the peaks. The appropriate differential equations[38] were integrated numerically and rate constants determined by a nonlinear optimization procedure using the program SCIENTIST (Version 2.0, MicroMath Inc.). The errors represent 1 standard deviation. In all cases, the data were fit using appropriate first- and second-order rate equations. Second-order rate constants are based on the concentration of Pt binding sites, which are in each case twice the concentration of duplex. In the cases of the cisplatin reactions, the initial concentration of *cis*-$[PtCl(^{15}NH_3)_2(OH_2)]^+$ was treated as 3% of the total platinum concentration. This was done because the cisplatin solution was heated to 310 K and was sonicated to aid dissolution of cisplatin. During the time used to dissolve the cisplatin, some hydrolysis of the Cl^- ligands in cisplatin could have occurred. Minima were found using simulations and by gradually optimizing the input parameters, fixing some while others were refined, and then finally allowing all parameters to be refined simultaneously.

Results

[^1H,^{15}N] HSQC 2D NMR spectroscopy has been used to study the rates of the reactions of the self-complementary sequences 5′-d(AATT**AG**TACTAATT)-3′ (-**AG**-) and 5′-d(AATT**GA**TATCAATT)-3′ (-**GA**-) with both *cis*-$[PtCl_2(^{15}NH_3)_2]$ and *cis*-$[Pt(^{15}NH_3)_2(OH_2)_2]^{2+}$. ^1H NMR spectra were also acquired to monitor oligonucleotide base-pairing through examination of the imino resonances ($\delta = 10-15$ ppm) and to verify Pt binding to N7 by means of the shifts of the purine H8 resonances ($\delta = 6.5-9.5$ ppm). The reaction conditions (9 mM phosphate, pH 6.0, 298 K for cisplatin and 0.1 M $NaClO_4$, pH 4.9, 288 K for *cis*-$[Pt(^{15}NH_3)_2(OH_2)_2]^{2+}$) were chosen to allow direct comparisons with the recently published studies of the kinetics of the reactions of cisplatin[26] and *cis*-$[Pt(^{15}NH_3)_2(OH_2)_2]^{2+}$(**2**)[27] with the 14-mer duplex 5′-d(ATACAT**GG**TACATA)-3′,5′-d(TATGTACCATGTAT)-3′ (hereafter -**GG**-). Examination of the temperature dependence of the imino ^1H shifts (melting profile) of the unplatinated -**AG**- and -**GA**- sequences confirmed that the self-complementary sequences are in the duplex form under the experimental conditions. The two sequences have almost identical melting temperatures, denaturing above 313 K. At 288 K, imino resonances attributed to all seven unique base-pair groupings are visible, whereas at 298 K the outermost AT base pairs are not resolved. The assignments of the imino protons and the melting profiles are discussed in detail elsewhere.[39]

The numbering scheme for the bases in the -**AG**- oligonucleotide is

1	2	3	4	5	6	7	8	9	10	11	12	13	14	
5′-d(	A	A	T	T	**A**	**G**	T	A	C	T	A	A	T	T)-3′

and in the -**GA**- oligonucleotide is

1	2	3	4	5	6	7	8	9	10	11	12	13	14	
5′-d(	A	A	T	T	**G**	**A**	T	A	T	C	A	A	T	T)-3′

Reaction of -AG- with Cisplatin. The reaction between cisplatin and -**AG**- was followed by [^1H,^{15}N] HSQC 2D NMR spectroscopy for a total of 140 h. Figure 1a shows a typical

(33) Piotto, M.; Saudek, V.; Sklenar, V. *J. Biomol. NMR* **1992**, *2*, 661−665.
(34) Stonehouse, J.; Shaw, G. L.; Keeler, J.; Laue, E. D. *J. Magn. Reson. Ser. A* **1994**, *107*, 174−184.
(35) Berners-Price, S. J.; Frenkiel, T. A.; Frey, U.; Ranford, J. D.; Sadler, P. J. *J. Chem. Soc., Chem. Commun.* **1992**, 789−791.
(36) Berners-Price, S. J.; Corazza, A.; Guo, Z.; Barnham, K. J.; Sadler, P. J.; Ohyama, Y.; Leng, M.; Locker, D. *Eur. J. Biochem.* **1997**, *243*, 782−791.
(37) Ismail, I. M.; Kerrison, S. J. S.; Sadler, P. J. *Polyhedron* **1982**, *1*, 57−59.
(38) The appropriate differential equations are provided as Supporting Information.
(39) Berners-Price, S. J.; Davies, M. S.; Jones, A. R.; Hambley, T. W. manuscript in preparation.

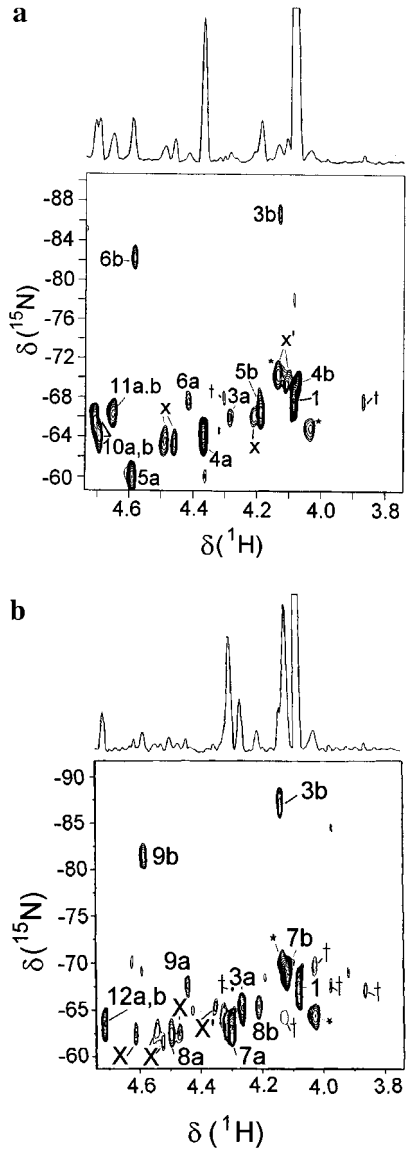

Figure 1. 2D [^{1}H,^{15}N] HSQC NMR (600 MHz) spectra at 298 K of (a) duplex -**AG**- after reaction with ^{15}N-cisplatin (**1**) for 12.8 h and (b) duplex -**GA**- after reaction with ^{15}N-cisplatin (**1**) for 13.3 h. Labels: ∗,^{195}Pt satellites; †, artifact; peaks are assigned to NH_3 in structures **1**−**12** (see Table 1). Peaks labeled x are assigned to other monofunctional adducts (for which the partner peaks x′ are close to or obscured by the ^{195}Pt satellite). For -**AG**- these are assumed to transform into other adducts which are obscured by the -**AG**- chelate peaks (**10** and **11**), see text. In each case, two major monofunctional adducts are observed, "G/Cl" (**4** and **7**) and "A/Cl" (**5** and **8**), as well as a monofunctional aqua species (**6** and **9**) which is assigned as "G/H_2O". Whereas for -**AG**- there are two conformers of the bifunctional -**AG**- chelate (**10** and **11**), there is only one conformation of the -**GA**- chelate (**12**). For both **11** and **12** the resonances for the two NH_3 groups are coincident under these conditions. Peaks labeled † are artifacts associated with the intense cisplatin peak and have been observed previously with use of this HSQC sequence.[26]

spectrum, in this case recorded after 12.8 h. Peak assignments and chemical shifts are listed in Table 1. The peaks were assigned on the basis of their appearance and disappearance, and on assignments from reactions between cisplatin and the 14-mer duplex -**GG**- reported by Berners-Price et al.[26] All species, other than cisplatin, are expected to give rise to two peaks (two nonequivalent NH_3 ligands), and by following the changes in their volumes with time it is possible to identify the pairs and make assignments on the basis of the expected reaction pathway and the ^{15}N shifts that are diagnostic of the trans ligand.[28−30] The course of the reaction is shown in Figure 2a, and the kinetic fits to the data give the rate constants that are defined in Scheme 1 and listed in Table 2.

Cisplatin first hydrolyzes to form *cis*-[PtCl($^{15}NH_3$)$_2$(OH_2)]$^+$ (**3**), which accounts for ∼2% of the total platinum until approximately 20 h has elapsed. Despite its low relative abundance, the aquachloro species is readily observed in the 2D NMR spectra (Figure 1a). Several monofunctional adducts are detected on reaction of *cis*-[PtCl($^{15}NH_3$)$_2$(OH_2)]$^+$ with the -**AG**- duplex, the dominant two assignable to G(6) and A(5) monofunctional adducts on the basis of the ^{1}H,^{15}N shifts of the NH_3 groups in comparison with those of monofunctional adducts in the reactions of cisplatin with -**GG**-[26] and the ^{1}H shifts of the H8 protons (vide infra). These adducts exhibit substantially different kinetic behavior; they form at different rates, and the adduct that is generated more slowly is longer lived. The most rapidly formed adduct, *cis*-[PtCl(N7G(6))($^{15}NH_3$)$_2$] (**4**), denoted here as "G/Cl", reaches a maximum relative concentration of about 25% of total platinum, while the more slowly formed of the two major adducts never exceeds ∼10% of the total platinum and is assignable to *cis*-[PtCl(N7A(5))($^{15}NH_3$)$_2$] ("A/Cl") (**5**). The G/Cl adduct ring closes more rapidly than the A/Cl adduct, the latter being still detectable after 140 h. This parallels the behavior of the 3′ G/Cl monofunctional adduct in the analogous reaction with -**GG**-.[26] At least three other minor intermediates are detected (Figure 1a), with ^{1}H,^{15}N shifts at ca. δ = (4.49/−63.7, 4.10/−68.5), (4.46/−63.4, 4.19/−66.5), and (4.21/−65.8, 4.13/−70.4). Their behavior suggests that they represent other minor monofunctional adducts in which the second NH_3 resonance lies near to or is obscured by that of the cisplatin peak or ^{195}Pt satellites. Small amounts of a monofunctional aqua adduct (**6**) are observed with ^{1}H,^{15}N shifts at δ = 4.57/−82.2 and 4.41/−67.5 in the period 1.5−40 h of reaction. This is assigned to the G monofunctional aqua adduct on the basis of the higher concentration of G/Cl relative to the other monofunctional adducts, as well as its more rapid formation.

Cisplatin has totally reacted after ∼65 h, at which time the dominant species is the Pt-**AG**- chelate. As observed previously[26] for the reaction of cisplatin with -**GG**-, the chelate product gives rise to two sets of ^{1}H,^{15}N cross-peaks in each spectrum, assignable to two conformational forms of the chelate product. As is the case for -**GG**-, these coexist in a temperature- and pH-dependent equilibrium, and this is examined in detail elsewhere.[39] For one form of -**AG**- chelate, both NH_3 peaks are resolved (δ = 4.69/−64.0, 4.70/−65.3) (**10**), whereas for the other form the two NH_3 resonances are coincident (δ = 4.65/−66.2) (**11**) under the conditions of this study (Figure 1a) but are resolved at 283 K.[39] The latter is the dominant form at high pH and low temperature, and it is noteworthy that, in the case of -**GG**-, the adduct that dominates under these conditions has distinct NH_3 shifts.[26] In the kinetic fits, the total chelate concentration has been used rather than those of the individual conformations because it is probable that equilibration occurs following closure. Peaks for the other monofunctional adducts are no longer visible after ∼40 h, and it is assumed that they transform to other products that are obscured by the -**AG**- chelate resonances. The contribution of these other products was estimated from the aromatic region of the ^{1}H spectra. The -**AG**- chelate peak (**10a** in Figure 3a) at 9.12 ppm is more intense than its partner at 8.97 ppm (**10b**). The difference in intensities between these two was found to be ∼10% of the total of platinated -**AG**- (sum of **10** and **11**). This was then

Table 1. ^{1}H and ^{15}N Chemical Shifts

species	label	pH[a]	temp (K)	δ ^{1}H	δ ^{15}N (trans ligand)
cis-[$PtCl_2(^{15}NH_3)_2$]	**1**	6.0	298	4.08	−67.8 (Cl)
cis-[$Pt(^{15}NH_3)_2(OH_2)_2]^{2+}$	**2**	4.9	288	4.54	−85.5 (O)
cis-[$PtCl(^{15}NH_3)_2(OH_2)]^{+}$	**3 (a)**	6.0	298	4.28	−65.7 (Cl)
	3 (b)			4.13	−87.3 (O)
		Monofunctional Adducts			
		-AG-			
cis-[PtCl(N7**G**(6))($^{15}NH_3)_2$]	**4 (a)**	6.0	298	4.36	−64.2 (N/Cl)
	4 (b)			4.07	−68.9 (Cl/N)
cis-[PtCl(N7**A**(5))($^{15}NH_3)_2$]	**5 (a)**	6.0	298	4.59	−60.0 (Cl/N)
	5 (b)			4.19	−67.3 (N/Cl)
cis-[Pt(N7**G**(6))($^{15}NH_3)_2(H_2O)$]	**6 (a)**	4.9	288	4.47	−67.7 (N)
	6 (b)			4.64	−82.5 (O)
cis-[Pt(N7**G**(6))($^{15}NH_3)_2(H_2O)$]	**6 (a)**	6.0	298	4.41	−67.5 (N)
	6 (b)			4.57	−82.2 (O)
		-GA-			
cis-[PtCl(N7**G**(5))($^{15}NH_3)_2$]	**7 (a)**	6.0	298	4.30	−63.7 (Cl/N)
	7 (b)			4.11	−68.2 (N/Cl)
cis-[PtCl(N7**A**(6))($^{15}NH_3)_2$]	**8 (a)**	6.0	298	4.50	−63.0 (Cl/N)
	8 (b)			4.21	−65.9 (N/Cl)
cis-[Pt(N7**G**(5))($^{15}NH_3)_2(H_2O)$]	**9 (a)**	4.9	288	4.49	−68.6 (N)
	9 (b)			4.61	−82.1 (O)
cis-[Pt(N7**G**(5))($^{15}NH_3)_2(H_2O)$]	**9 (a)**	6.0	298	4.44	−68.6 (N)
	9 (b)			4.58	−81.6 (O)
		Bifunctional Adducts			
		-AG- (Two Conformers)			
cis-[Pt(N7**A**(5))(N7**G**(6))($^{15}NH_3)_2$]	**10 (a)**	6.0	298	4.69	−64.0 (N)
	10 (b)			4.70	−65.3 (N)
cis-[Pt(N7**A**(5))(N7**G**(6))($^{15}NH_3)_2$]	**10 (a)**	4.9	288	4.73	−65.7 (N)
	10 (b)			4.71	−64.3 (N)
cis-[Pt(N7**A**(5))(N7**G**(6))($^{15}NH_3)_2$]	**11 (a)/(b)**	6.0[b]	298	4.65	−66.2 (N)
cis-[Pt(N7**A**(5))(N7**G**(6))($^{15}NH_3)_2$]	**11 (a)/(b)**	4.9[b]	288	4.68	−66.3 (N)
		-GA- (One Conformer)			
cis-[Pt(N7**G**(5))(N7**A**(6))($^{15}NH_3)_2$]	**12**[a]	6.0[b]	298	4.71	−64.2 (N)
cis-[Pt(N7**G**(5))(N7**A**(6))($^{15}NH_3)_2$]	**12 (a)**	4.9	288	4.74	−64.4 (N)
	12 (b)			4.79	−65.6 (N)

[a] Conditions for pH 6.0, 9 mM $NaPO_4^{3-}$, and for pH 4.9, 0.1 M $NaClO_4$. [b] The two $-NH_3$ resonances are overlapped under these conditions.

taken into account in determining the ^{1}H,^{15}N peak volumes for the **-AG-** chelate.

Evidence for formation of both G and A monofunctional adducts is obtained from the detection of resonances for the H8 protons in the ^{1}H spectrum. For double-stranded B-DNA, the ^{1}H signals of the H8 protons of A and G bases are confined to the 8.0−8.4- and 7.6−8.0-ppm regions, respectively,[40] and the inductive effects due to binding of *cis*-$\{Pt(NH_3)_2\}^{2+}$ have been determined recently as 0.68 ± 0.02 (for A) and 0.52 ± 0.01 ppm (for G).[41] Assuming that for monofunctional adducts the deshielding of the H8 resonances on coordination of Pt to N7 will mainly reflect the inductive effect, then for G/Cl the H8 proton is expected to occur in the region 8.1−8.5 ppm, whereas for A/Cl the H8 will be more strongly deshielded in the region 8.7−9.1 ppm. Figure 3a shows the time dependence of the H8 region of the ^{1}H spectrum of the **-AG-** duplex on reaction with cisplatin. A new peak appears at 8.92 ppm, and a more intense new peak appears at 8.26 ppm, with time dependences that parallel those of the Pt−NH_3 peaks for the A/Cl and G/Cl monofunctional adducts **5** and **4**, respectively, in the [^{1}H,^{15}N] spectra.[42] The H8 region of the ^{1}H spectrum shows also two sets of signals for the two conformational forms of **-AG-** chelate (**10** and **11**) (Figure 3a), consistent with the results obtained from the [^{1}H,^{15}N] spectra.

There are several notable changes in the imino region of the ^{1}H spectra during the course of the reaction (Figure 4a). Resonances indicative of monofunctional platinum adducts appear then disappear, most notably in the region between the AT and GC imino resonances (δ = 12.7−13.2) of the free **-AG-** oligonucleotide.

Reaction of -GA- with Cisplatin. Treatment of the **-GA-** duplex with cisplatin at 298 K, pH 6.0, in sodium phosphate-buffered solution sees a slow reaction occur. Only after more than 100 h is all of the cisplatin consumed. A typical [^{1}H,^{15}N] spectrum recorded after 13.3 h is shown in Figure 1b, and peak assignments and chemical shifts are listed in Table 1.

In the first step, cisplatin hydrolyzes to form *cis*-[$PtCl(^{15}NH_3)_2(OH_2)]^{+}$ (**3**), which accumulates to approximately 9% of the total Pt, considerably higher than the 2−3% found for the same species in the analogous reaction with **-AG-**. The initial hydrolysis of cisplatin is normally the rate-determining-step in such reactions, but in this case the formation of the monofunctional adducts from the aqua-chloro species is also a slow process. This is further evidenced by the rate of disappearance of cisplatin in the reaction with **-GA-** being approximately two-thirds that observed with **-AG-**. These two factors clearly indicate that binding of *cis*-$[PtCl(NH_3)_2(OH_2)]^{+}$ to the **-GA-** oligonucleotide is considerably slower than that observed with the **-AG-** oligonucleotide. As for the reaction with **-AG-**, resonances assignable to both G/Cl (**7**) and A/Cl (**8**) as well as other minor monofunctional adducts are seen (Figure 1b). The most abundant adduct is assignable as *cis*-[PtCl(N7G(5))($^{15}NH_3)_2$], (G/Cl) (**7**) on the basis of the ^{1}H,^{15}N

(40) van de Ven, F. J. M.; Hilbers, C. W. *Nucleic Acids Res.* **1988**, *16*, 5713−5726.

(41) Lemaire, D.; Fouchet, M.-H.; Kozelka, J. *J. Inorg. Biochem.* **1994**, *53*, 261−271.

(42) A plot of the time dependences of the H8 resonances for the cisplatin + -AG- reaction is provided as Supporting Information.

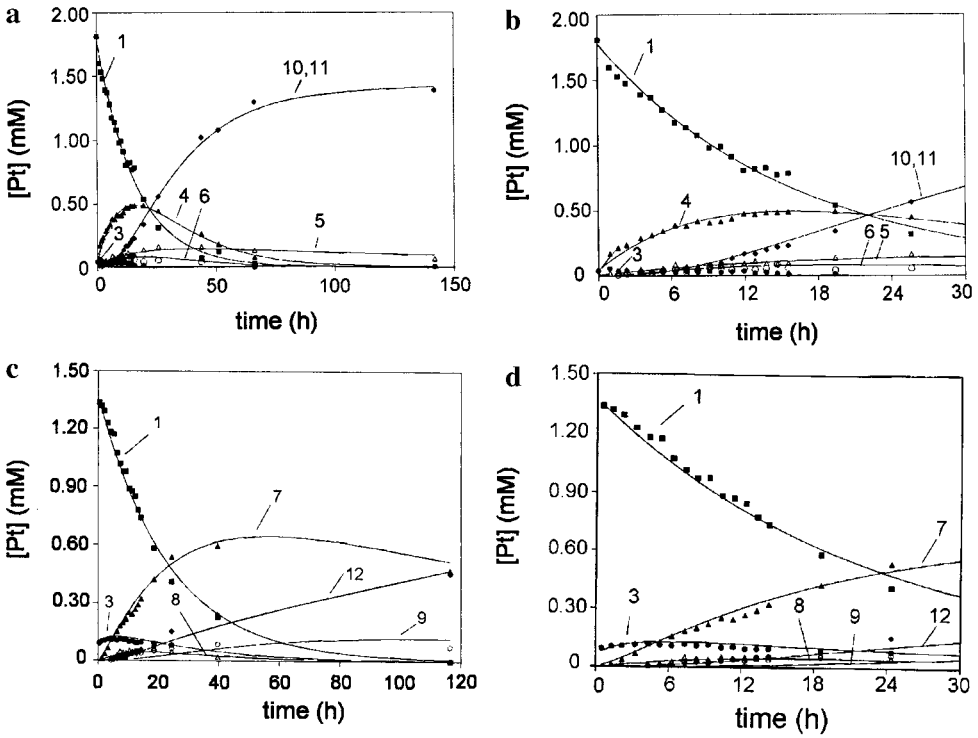

Figure 2. Plots of relative concentration of species observed during reactions at 298 K between (a) -**AG**- and ^{15}N-cisplatin (**1**) (labels: ■, **1**; ●, **3**; ▲, **4**; △, **5**; ○, **6**; ◆, **10** + **11**; for the purposes of the fit the sum of concentrations of the two forms of -**AG**- chelate was used) and (b) -**GA**- and ^{15}N-cisplatin (**1**) (labels: ■, **1**; ●, **3**; ▲, **7**; △, **8**; ○, **9**; ◆, **12**). The curves are computer best fits for the rate constants shown in Table 2, and species labeled are defined in Table 1.

Scheme 1. Kinetic Pathway for the Reaction between ^{15}N-Cisplatin and -**AG**-[a]

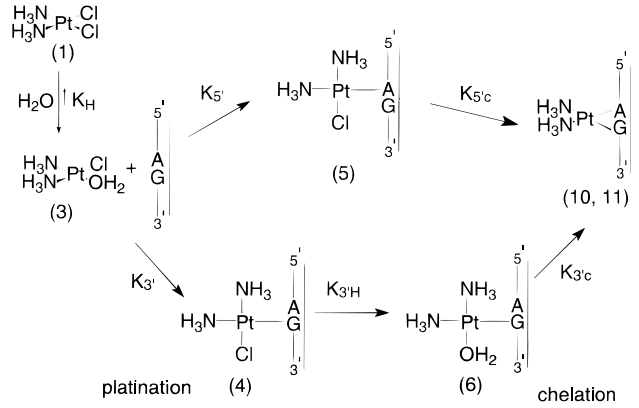

[a] The analogous scheme for -**GA**- is not shown. The data were also analyzed without inclusion of the G/H_2O intermediate (Table 2).

shifts (δ = 4.30/−63.7, 4.11/−68.2), which are similar to those of the 5'-G monofunctional adduct of the -**GG**- duplex.[26] The second most abundant adduct has ^{1}H,^{15}N shifts at δ = 4.21,−65.9 and 4.50,−63.0, and this is assigned as *cis*-[PtCl(N7A-(6))($^{15}NH_3$)$_2$] (A/Cl) (**8**) (Table 1).

The G/Cl adduct appears within 0.5 h, reaching a maximum concentration of ∼45% total platinum after ∼50 h, and then decreases as ring closure to form the chelate becomes significant. After 117 h, some 35% of the total Pt remains in the form of this monofunctional adduct. The A/Cl monofunctional adduct is shorter lived, appearing after 4 h and becoming undetectable between 25 and 117 h. Closure of the G/Cl adduct to form the -**GA**- chelate is substantially slower than is formation of the -**AG**- chelate, as evidenced by the buildup of the monofunctional adduct. In addition, a monofunctional aqua adduct with ^{1}H,^{15}N shifts of δ = 4.58/−81.6 and 4.44/−68.6 is seen after 6 h, still observed at 40 h but not detected at 117 h of the experiment.

The onset of detection of the -**GA**- chelate is at ∼8 h, and it builds slowly so that after ∼117 h the chelate adduct accounts for only ∼35% of total Pt. In contrast to the -**AG**- reaction, only one platinum -**GA**- chelate conformation is observed. This species exhibits pH-dependent chemical shifts so that, at pH 6.0, only one ^{1}H,^{15}N resonance is apparent (δ = 4.71/−64.2, Figure 1b), but at pH 4.9 distinct ^{1}H,^{15}N resonances for the two NH_3 groups are resolved (δ = 4.74/−64.4 and 4.79/−65.6, Figure 5b). After ∼6 h, several new peaks begin to appear, e.g., with ^{1}H,^{15}N shifts at δ = 4.47/−63.8, 4.35/−65.7, 4.48/−63.1, 4.19/−68.0, and 4.61/−62.8. These are assumed to correspond to other monofunctional adducts, but, in contrast to the reaction with -**AG**-, it was not possible to identify separate pairs of resonances on the basis of their time-dependent behavior. These other monofunctional species are estimated to account for at least 15% of the total Pt at 18 h. Some of these adducts appear to convert into a product that has ^{1}H,^{15}N shifts at δ = 4.53/−63.9. This species represents ∼13% of the total platinum at 117 h. After 25 days, in addition to this peak there were at least four other resonances present with ^{1}H,^{15}N shifts in the range from 4.4 to 4.6/−63 to −65 ppm, corresponding to either monofunctional adducts or final products. These unidentified species represented ∼30% of the total Pt-NH_3 species present and may indicate that the G/Cl monofunctional adduct forms other products in addition to the -**GA**- chelate. Despite the complication of formation of other products, good fits to the data defined in Scheme 1 were obtained. The time dependence of the concentration of species in the reaction is shown in Figure 2b, and the rate constants obtained from the kinetic fits are listed in Table 2.

The time dependence of the aromatic region of the ^{1}H spectra obtained during the course of the reaction between -**GA**- and

Table 2. Rate Constants for the Reactions between -**AG**- and -**GA**- with *cis*-[$PtCl_2(^{15}NH_3)_2$] at 298 K, pH 6.0[a]

	-**AG**- + cisplatin		-**GA**- + cisplatin		
rate constant	incl G/H_2O (**6**)	no G/H_2O	incl G/H_2O (**9**)	no G/H_2O	-**GG**- + cisplatin[b]
$K_H/10^{-5}$ s^{-1}	1.706 ± 0.014	1.71 ± 0.03	1.13 ± 0.03	1.13 ± 0.02	1.83 ± 0.03
$K_{3'}/M^{-1}$ s^{-1}	1.06 ± 0.06	0.96 ± 0.07	0.0054 ± 0.0010	0.0054 ± 0.0007	0.47 ± 0.04
$K_{5'}/M^{-1}$ s^{-1}	0.149 ± 0.014	0.139 ± 0.017	0.023 ± 0.002	0.0228 ± 0.0009	0.15 ± 0.03
$K_{3'H}/10^{-5}$ s^{-1}	1.55 ± 0.05		*		
		1.59 ± 0.05		2.1 ± 0.5	3.2 ± 0.1
$K_{3'C}/10^{-5}$ s^{-1}	9.8 ± 0.9		2.1 ± 0.7		
$K_{5'H}/10^{-5}$ s^{-1}	*		0.198 ± 0.008		
		0.18 ± 0.07		0.198 ± 0.016	0.24 ± 0.18
$K_{5'C}/10^{-5}$ s^{-1}	0.16 ± 0.06		0.69 ± 0.17		

[a] The -**AG**- and -**GA**- reactions were modeled as going through the G/H_2O species prior to ring closure. No analogous data are available for -**GG**-. For comparison, the -**AG**- and -**GA**- reactions were also modeled without the G/H_2O intermediate; rate constants so determined are listed in columns 3 and 5 for -**AG**- and -**GA**-, respectively. An * indicates "not observed". [b] From ref 26.

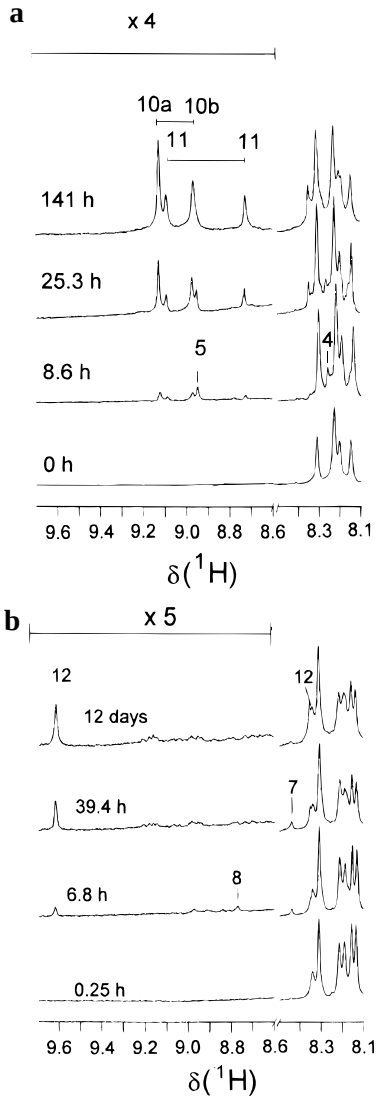

Figure 3. ^1H NMR (600 MHz) spectra at 298 K of the time dependence of the aromatic regions of (a) -**AG**- and (b) -**GA**- on reaction with *cis*-[$Pt(^{15}NH_3)_2Cl_2$] (**1**). The peaks are assigned to guanine and adenine H8 protons in the "G/Cl" (**4**, **7**) and "A/Cl" (**5**, **8**) monofunctional adducts and the bifunctional chelates (-**AG**-, **10** and **11**; -**GA**-, **12**). The intensity of the peak at 9.12 ppm (**10a** in a) is heightened by the contribution of "other products". In the -**GA**- reaction, other products give rise to minor peaks in the 8.5−9.3-ppm region. In both spectra, the region 8.6−9.7 ppm is plotted at 4 (a) or 5 (b) times the intensity of the 8.1−8.5-ppm region.

cisplatin is shown as Figure 3b. A deshielded resonance at 8.44 ppm is assignable to the G(5) H8 of the G/Cl monofunctional

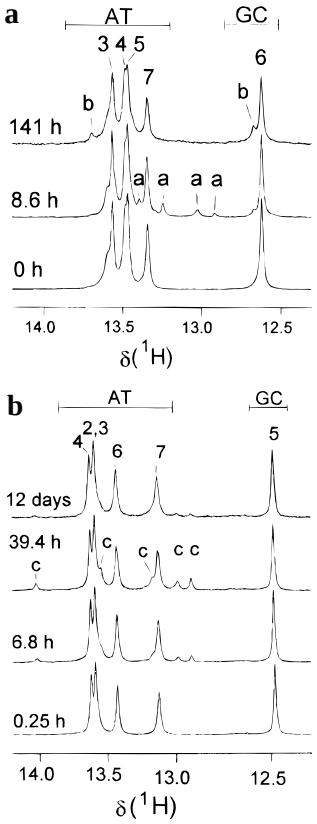

Figure 4. ^1H NMR (600 MHz) spectra at 298 K of the time dependence of the imino regions of (a) -**AG**- and (b) -**GA**- on reaction with *cis*-[$Pt(^{15}NH_3)_2Cl_2$] (**1**). Assignments of resonances to base pairs are indicated by numbers (1 = A(1)-T(14), etc.), and letters indicate assignments to platinated duplexes: a, **4**/**5**; b, **10**/**11**; c, **7** (see Table 1 for assignments).

adduct **7** on the basis of the intensity profile that mirrors that obtained for this species in the [^1H,^{15}N] spectrum. A second weak resonance at δ = 8.77 is seen in the first 40 h and is tentatively assigned to A/Cl (**8**). Two new resonances appear at 9.62 and 8.35 ppm that are assignable to the H8 resonances of the Pt-**GA**- chelate. As seen in the [^1H,^{15}N] spectra, and in contrast to the -**AG**- platinated duplex, a single set of resonances indicating only one conformer of Pt-**GA**- chelate is observed. The H8 region shows also numerous small peaks in the region 9.3−8.6 ppm. No definite assignments could be made on any peak in this region due to the low intensity of the signals. However, the presence of this multitude of small peaks is consistent with the [^1H,^{15}N] spectra where a large number of minor monofunctional and product species are observed.

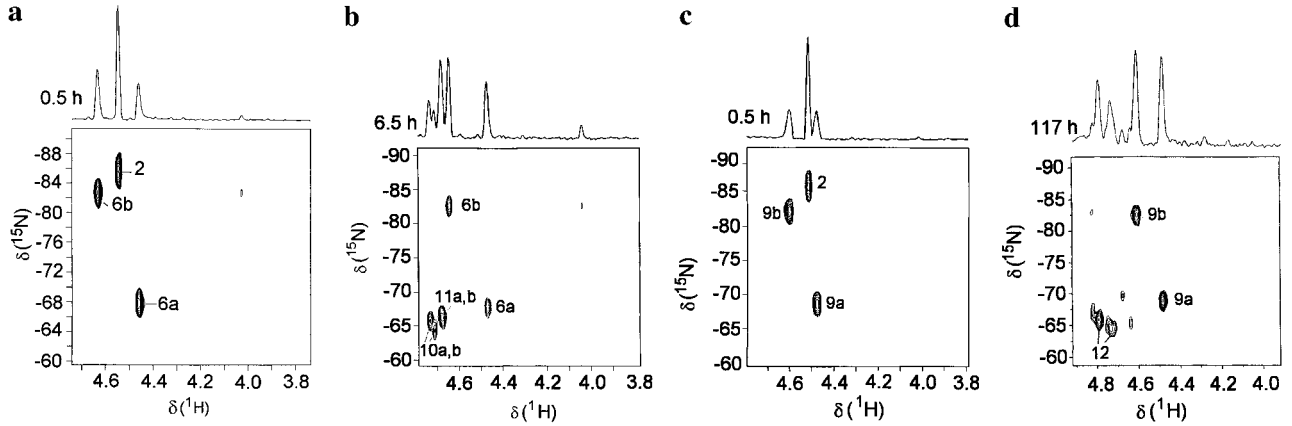

Figure 5. 2D [^{1}H,^{15}N] HSQC NMR (600 MHz) spectra at 288 K of duplex -**AG**- after reaction with *cis*-[Pt(^{15}NH$_3$)$_2$(OH$_2$)$_2$]$^{2+}$ (**2**) for (a) 0.15 and (b) 6.5 h and duplex -**GA**- after reaction with *cis*-[Pt(^{15}NH$_3$)$_2$(OH$_2$)$_2$]$^{2+}$ (**2**) for (c) 0.15 and (d) 117 h. Peaks are assigned to NH$_3$ in the G/H$_2$O monofunctional adducts **6** and **9** and the bifunctional chelates **10**, **11** (-**AG**-), and **12** (-**GA**-) (for assignments see Table 1). The ^{1}H,^{15}N shifts of the -**GA**- chelate (**12**) are pH dependent, so at this pH distinct resonances are resolved for the two NH$_3$ groups, whereas at pH 6.0 the two resonances are overlapped (see Figure 1b).

The imino region of the ^{1}H spectrum shows several distinct changes on reaction of -**GA**- with cisplatin. In Figure 4b, five resonances attributable to the G/Cl monofunctional adduct are seen; most notably, a resonance observed at δ =14.01 is strongly deshielded with respect to all the imino resonances for the unreacted -**GA**- duplex, suggesting that the G/Cl monofunctional adduct strongly distorts the structure of the -**GA**- duplex.

Reaction of -AG- with *cis*-[Pt(^{15}NH$_3$)$_2$(OH$_2$)$_2$]$^{2+}$. The overall reaction between *cis*-[Pt(^{15}NH$_3$)$_2$(OH$_2$)$_2$]$^{2+}$ and -**AG**- at 288 K, pH 4.9, in 0.1 M NaClO$_4$ is significantly more rapid than the equivalent reaction with cisplatin but is slower than that observed by Reeder et al.[27] in similar reactions with -**GG**-. Formation of the monofunctional G/H$_2$O adduct from *cis*-[Pt(^{15}NH$_3$)$_2$(OH$_2$)$_2$]$^{2+}$ is slower than formation of the G/Cl adduct in the cisplatin reaction from *cis*-[PtCl(^{15}NH$_3$)$_2$(OH$_2$)]$^+$, but allowing for changes in pH and temperature, the rates are probably similar. Over the course of 1 h, the concentration of *cis*-[Pt(^{15}NH$_3$)$_2$(OH$_2$)$_2$]$^{2+}$ diminishes with the formation of *cis*-[Pt(N7G(6))(^{15}NH$_3$)$_2$(OH$_2$)]$^+$ (G/H$_2$O) (**6**). Typical [^{1}H,^{15}N] HSQC 2D NMR spectra are shown in Figure 5a/b. In contrast to the reaction with cisplatin, a second (A-bound) monofunctional adduct is not observed. The [^{1}H,^{15}N] spectra provide some evidence of a second monofunctional species (A/H$_2$O) since a minor shoulder (δ = 4.66/−82.5) is observed to the high-frequency side of the major G/H$_2$O peak (δ = 4.64/−82.5) during the first 6 h of the reaction. However, no second peak was detected for the other NH$_3$ group, and the relative intensity of the second G/H$_2$O peak (δ = 4.47/−67.7) is not consistent with overlap of another peak. In addition, there is no resonance in the H8 region of the ^{1}H spectra that has a shift and time dependence in accord with Pt coordinated to N7 of adenine. It seems likely, therefore, that the ^{1}H,^{15}N peak at δ = 4.66/−82.5 is an artifact, perhaps due to the proximity of the ^{1}H$_2$O resonance.

As observed in the reaction with cisplatin, two conformational forms of the -**AG**- chelate product are seen (**10**) and **11**) (Figure 5b), and for the purposes of the kinetic fit, the sum of the concentrations was used. The results of the kinetic fits to the data are presented in Figure 6a, and the parameters defined in Scheme 2 are listed in Table 3.

Reaction of -GA- and *cis*-[Pt(^{15}NH$_3$)$_2$(OH$_2$)$_2$]$^{2+}$. As for the reaction with the -**AG**- duplex, one (G/H$_2$O) monofunctional adduct is observed in the [^{1}H,^{15}N] spectra of the reaction of -**GA**- and *cis*-[Pt(^{15}NH$_3$)$_2$(OH$_2$)$_2$]$^{2+}$ (**2**) (Figure 5c/d). The rate of loss of *cis*-[Pt(^{15}NH$_3$)$_2$(OH$_2$)$_2$]$^{2+}$ is similar in the reactions

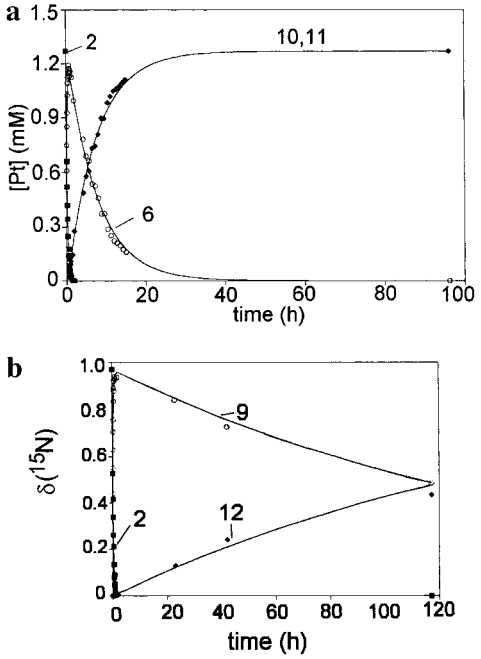

Figure 6. Plots of relative concentration of species observed during reactions at 288 K between (a) -**AG**- and *cis*-[Pt(^{15}NH$_3$)$_2$(OH$_2$)$_2$]$^{2+}$ (**2**) (labels: ■, **2**; ○, **6**; ◆, **10** + **11**; for the purposes of the fit the sum of concentrations of the two forms of -**AG**- chelate was used and (b) -**GA**- and *cis*-[Pt(^{15}NH$_3$)$_2$(OH$_2$)$_2$]$^{2+}$ (**2**). (labels: ■, **2**; ○, **9**; ◆, **12**). The curves are computer best fits for the rate constants shown in Table 3.

with the -**AG**- and -**GA**- duplexes, in contrast to the rate of disappearance of cisplatin and the rate of formation of monofunctional adducts in the cisplatin reactions. As shown in Figure 6b, ring closure from the G/H$_2$O monofunctional in -**GA**- is greatly slowed relative to that in -**AG**-, and as found for the reaction of -**GA**- with cisplatin, only one conformation of the chelate is observed. Minor species with ^{1}H,^{15}N peaks at δ = 4.66/−69.3 and 4.61/−65.0 are observed late in the reaction. The kinetic fits to the data presented in Figure 6b and rate constants are listed in Table 3.

As observed in the reaction of -**GA**- with cisplatin, the imino region of the ^{1}H spectrum shows changes that indicate that the G/H$_2$O monofunctional adduct strongly distorts the structure of the -**GA**- duplex in the platination region (Figure 7b). In addition to the strongly deshielded resonance at δ = 14.1, also

Scheme 2. Kinetic Pathway for the Reaction between *cis*-[Pt($^{15}NH_3$)$_2$(OH$_2$)$_2$]$^{2+}$ and -**AG**-[a]

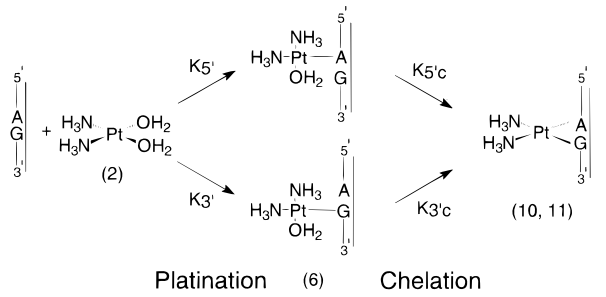

[a] The analogous scheme for -**GA**- is not shown. Note that monofunctional A adducts were not detected in the NMR spectra for either the -**AG**- or -**GA**- reactions.

observed in the reaction with cisplatin, after 0.45 h a new peak is apparent at $\delta = 10.85$, which is within the region characteristic of non-Watson−Crick H-bonded bases.[43] This peak is not observed after 12 days and is, therefore, clearly assignable to the G/H$_2$O monofunctional adduct. It was not observed in the reaction of -**GA**- with cisplatin, which is presumably a consequence of more rapid exchange with solvent at the higher temperature. In the reaction of *cis*-[Pt($^{15}NH_3$)$_2$(OH$_2$)$_2$]$^{2+}$ with -**AG**-, a monofunctional species exhibits a peak at $\delta = 10.31$, and an imino resonance assignable to the -**AG**- chelate is seen at $\delta = 11.46$ in the latter stages of the reaction (Figure 7a).

Discussion

Hydrolysis of Cisplatin. The rate of hydrolysis of cisplatin to *cis*-[PtCl(NH$_3$)$_2$(OH$_2$)]$^+$ decreases from -**GG**- to -**AG**- to -**GA**-. The hydrolysis reaction was modeled as both an irreversible and a reversible first-order reaction. The reaction rate constant from the reversible model gave nonsensible results, and so the reaction was treated as irreversible. Consequently, the rates of hydrolysis reflect, in part, the rate of removal of *cis*-[PtCl(NH$_3$)$_2$(OH$_2$)]$^+$ from solution, which decreases in the same sequence (vide infra).

Monofunctional Binding of Cisplatin. The binding of cisplatin to the sequence 5′-d(ATACAT**GG**TACATA)-3′,5′-d(TATGTACCATGTAT)-3′ (-**GG**-) has been reported previously,[26] and the reported rate constants are listed in Table 2. In that case and in the present example, the target purine-purine sequence is surrounded by thymine bases making comparison of these three TPuPuT sequences a valid exercise.

Monofunctional adduct formation at the -**GG**- site shows a 3-fold preference for the 3′-G over the 5′-G;[24,27] thus, there is evidently an inherent preference for the 3' base in a TPuPuT sequence. In the case of the -**AG**- sequence, the G might be expected to be preferred on two counts: the kinetic preference for G over A[12−17] and the preference for the 3′ base. In accord with this, the preference for the 3′ base over the 5′ base is 7-fold, substantially greater than that observed for -**GG**-. The rate of binding to the guanine of -**AG**- is increased relative to binding to the 3′-G of -**GG**-; thus, it is not inhibited by the presence of an adenine on the 5′ side. Binding to the adenine of -**AG**- is similar to that of the 5′ G of -**GG**-. Thus, it appears that the presence of a guanine on the 3′ side considerably increases the binding to adenine over what would be expected to an isolated base.

(43) Wijmenga, S. S.; Mooren, M. M. W.; Hilbers, C. W. NMR of nucleic acids: from spectrum to structure. In *NMR of Macromolecules − A practical approach*; Roberts, G. C. K., Ed.; Oxford University Press: Oxford, UK, 1993; pp 217−288.

Monofunctional binding of *cis*-[PtCl(NH$_3$)$_2$(OH$_2$)]$^+$ to the -**GA**- sequence occurs at a greatly diminished rate compared to those of both -**GG**- and -**AG**-. The rate of binding to the 3′ base, the preferred site of attack in -**GG**- and -**AG**-, is 80−200-fold lower than for these sequences. This is slower than what is to be expected on the basis of the rates of binding to guanine and adenine.[13−17] Thus, the presence of the guanine on the 5′ side does not enhance binding at the adenine of -**GA**-. Binding to the 5′ guanine occurs at only one-sixth the rate of binding to the 5′-G of -**GG**-; thus, the presence of the adenine on the 3′ side adversely influences binding at the 5′ side. Indeed, the rate of binding is substantially less than that to the adenine of -**AG**-.

Bifunctional Adducts Formed by Cisplatin. The observation of aqua monofunctional adducts in both the reactions of -**AG**- and -**GA**- with cisplatin is important for determining the mechanism of ring closure; viz., does G/Cl ring close directly to the -**AG**- or -**GA**- chelate, or does it first hydrolyze to a G/H$_2$O intermediate? The results presented herein, and in particular the rate constants for the two steps, indicate that the G/H$_2$O intermediate plays a role in the mechanism of formation of the chelate species. The presence of a peak for the G/H$_2$O species (**6** or **9**) could arise either if the rate of monofunctional adduct formation is sufficiently slow that there is some further hydrolysis to *cis*-[Pt($^{15}NH_3$)$_2$(OH$_2$)$_2$]$^{2+}$, which reacts rapidly with the duplex, or if the rate of hydrolysis of the Cl$^-$ ligand in G/Cl is comparable to the overall rate of ring closure. For both reactions, it has been modeled here as the latter, based on the absence of a peak indicative of *cis*-[Pt($^{15}NH_3$)$_2$(OH$_2$)$_2$]$^{2+}$ in the [^{1}H,^{15}N] spectrum and the greater reactivity at Pt of Cl$^-$ and purine bases over H$_2$O.

Closure of the monofunctional adducts to give bifunctional adducts also varies across the three sequences. Since no equivalent data are available for -**GG**-, the two reactions were also modeled without involving the G/H$_2$O intermediate. For -**GG**-, closure from the 3′ adduct is 13 times faster than closure from the 5′ adduct, but in the -**AG**- case the ratio is 9:1. Closure from the 3′ adduct of -**AG**- might be expected to be slower because it involves binding to adenine, and this probably contributes to the reduction in the ratio. The rates of closure from the 5′ base are the same (within experimental errors) for -**GG**-, -**AG**-, and -**GA**- and are an order of magnitude slower than closure from the 3′ base. In the latter case, closure is fastest for -**GG**-, followed by -**GA**- and -**AG**-. Thus, it is clear that structural factors play a major role in determining the rates of these processes and can outweigh the inherent kinetic preference for binding to guanine over adenine.

Binding of *cis*-[Pt($^{15}NH_3$)$_2$(OH$_2$)$_2$]$^{2+}$ to -AG- and -GA-. Monofunctional binding of *cis*-[Pt($^{15}NH_3$)$_2$(OH$_2$)$_2$]$^{2+}$ to DNA is expected to be substantially more rapid than is binding to cisplatin because of the dipositive charge on the complex, the greater lability of the aqua ligand over Cl$^-$, and the circumvention of the initial hydrolysis step. This is, indeed, the case for the binding of *cis*-[Pt($^{15}NH_3$)$_2$(OH$_2$)$_2$]$^{2+}$ to -**GG**-, which is too rapid to measure reliably using [^{1}H,^{15}N] HSQC 2D NMR spectroscopy.[27] Binding to -**AG**- and **GA**- is slow enough to measure, and similar values are obtained for the two sequences. This contrasts strongly with the situation for cisplatin, where binding to -**AG**- is nearly an order of magnitude faster than binding to -**GA**-. Allowing for temperature and pH differences, the rates of binding of *cis*-[PtCl($^{15}NH_3$)$_2$(OH$_2$)]$^+$ and *cis*-[Pt($^{15}NH_3$)$_2$(OH$_2$)$_2$]$^{2+}$ to -**AG**- are similar, but binding of *cis*-[Pt($^{15}NH_3$)$_2$(OH$_2$)$_2$]$^{2+}$ is much faster than that of *cis*-[PtCl($^{15}NH_3$)$_2$(OH$_2$)]$^+$ to -**GA**-.

Table 3. Rate Constants for the Reactions of **-AG-** and **-GA-** with *cis*-[Pt($^{15}NH_3$)$_2$(OH$_2$)$_2$]$^{2+}$ at 288 K, pH 4.9

rate constant	**-AG-** + *cis*-[Pt($^{15}NH_3$)$_2$(OH$_2$)$_2$]$^{2+}$	**-GA-** + *cis*-[Pt($^{15}NH_3$)$_2$(OH$_2$)$_2$]$^{2+}$	**-GG-** + *cis*-[Pt($^{15}NH_3$)$_2$(OH$_2$)$_2$]$^{2+}$ [a]
$K_{3'}$/M^{-1} s^{-1}	0.419 ± 0.009	not observed	too fast to measure
$K_{5'}$/M^{-1} s^{-1}	not observed	0.5001 ± 0.007	too fast to measure
$K_{3'C}$/10^{-5} s^{-1}	3.71 ± 0.05	not observed	25 ± 3
$K_{5'C}$/10^{-5} s^{-1}	not observed	0.162 ± 0.005	4.9 ± 0.4

[a] From ref 27.

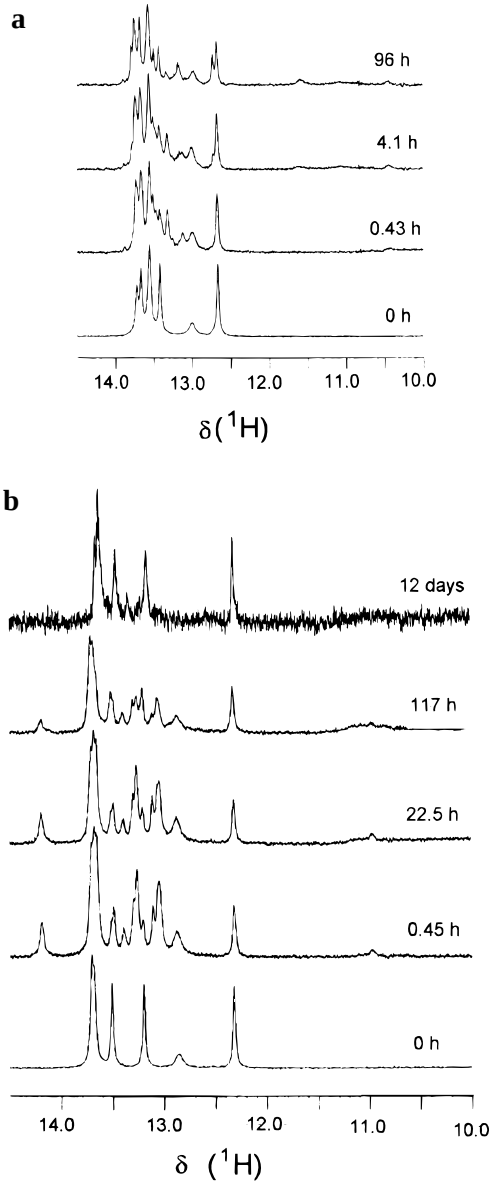

Figure 7. ^{1}H NMR (600 MHz) spectra at 288 K of the time dependence of the imino regions of (a) **-AG-** and (b) **-GA-** on reaction with *cis*-[Pt($^{15}NH_3$)$_2$(OH$_2$)$_2$]$^{2+}$ (**2**). The spectrum for **-GA-** at 12 days was recorded at 298 K.

It appears from these results that the adjacent bases do not have as pronounced an affect on the DNA binding of *cis*-[Pt($^{15}NH_3$)$_2$(OH$_2$)$_2$]$^{2+}$ as is the case for cisplatin. Binding of Pt to DNA is known to be kinetically determined, and Elmroth and Lippard[44] have shown that outer-sphere complex formation also influences the rate of adduct formation. Thus, the differences in the selectivities of cisplatin and *cis*-[Pt($^{15}NH_3$)$_2$(OH$_2$)$_2$]$^{2+}$ may be a consequence of either the more rapid binding of *cis*-[Pt($^{15}NH_3$)$_2$(OH$_2$)$_2$]$^{2+}$ leading to a reduced opportunity for outer-sphere complex formation to influence the reaction, or to differences in the nature of the interactions formed by *cis*-[PtCl($^{15}NH_3$)$_2$(OH$_2$)]$^+$ and *cis*-[Pt($^{15}NH_3$)$_2$(OH$_2$)$_2$]$^{2+}$ in the outer-sphere complexes or in the transition states.

The G/H$_2$O monofunctional adduct with **-GA-** is more prevalent under these reaction conditions than is the G/Cl adduct in the reaction between **-GA-** and cisplatin because of the large discrepancy between the rate of formation and the rate of ring closure of the G/H$_2$O adduct. This disparity is less pronounced with G/Cl because the rate of formation of G/Cl from cisplatin is relatively slow, being dependent first on the hydrolysis of cisplatin.

Rates of closure of *cis*-[Pt($^{15}NH_3$)$_2$(OH$_2$)$_2$]$^{2+}$-generated monofunctional adducts to form the bifunctional adducts are remarkably different for the three sequences. For **-GG-**, the closure rates for *cis*-[Pt($^{15}NH_3$)$_2$(OH$_2$)$_2$]$^{2+}$ are greater in magnitude but show a selectivity similar to those for cisplatin. Thus, closure from the 3′ monofunctional adduct is 5-fold faster than that from the 5′ adduct. For **-AG-** and **-GA-** closure is only observed from the G base. For **-AG-**, this is the 3′ side, and the rate is approximately 2−3 times faster for *cis*-[Pt($^{15}NH_3$)$_2$(OH$_2$)$_2$]$^{2+}$ than for cisplatin. For **-GA-**, the closure rate is more than an order of magnitude slower than the rate for **-AG-** and is similar to that observed for closure of the cisplatin-generated adduct on **-GA-** when modeled without involving the hydrolysis step to the G/H$_2$O species. Thus, ignoring pH and temperature differences, it emerges that *cis*-[Pt($^{15}NH_3$)$_2$(OH$_2$)$_2$]$^{2+}$ initially reacts at a rate comparable to that of *cis*-[PtCl($^{15}NH_3$)$_2$(OH$_2$)]$^+$ with **-AG-** and approximately 25 times faster with **-GA-** than *cis*-[PtCl($^{15}NH_3$)$_2$(OH$_2$)]$^+$. Closure to the **-AG-** chelate is twice as fast in the reaction from the *cis*-[Pt($^{15}NH_3$)$_2$(OH$_2$)$_2$]$^{2+}$ species than from cisplatin, but the rates are similar for **-GA-**.

Conclusions

The primary goal in undertaking this work was to determine rates for the reactions of cisplatin and *cis*-[Pt(NH$_3$)$_2$(OH$_2$)$_2$]$^{2+}$ with ApG and GpA sites so that they could be compared with the rates of reaction at GpG sites and shed light on the factors that influence Pt/DNA interactions and prevent formation of the bifunctional GpA adduct. The sequences analyzed were all of the form TpPupPupT (Pu = purine) and hence are directly comparable, but general conclusions must be tempered by the caveat that altering the flanking bases could significantly alter the reaction rates.

Comparison of the rates of the initial reaction of cisplatin with the three sequences leads to the tentative conclusion that the purine base on the 3′ side of the pair exerts a substantially greater influence on the rate of binding at the 5′ base than does the 5′ base on the rate of binding at the 3′ base. Clearly, this deserves further investigation by variation of the bases flanking the purine-purine target site, but results obtained by Chottard et al.[23,24] do confirm that the base on the 3′ site of a GpG pair exerts a substantial influence on the rates of binding at this site. These observations may indicate that the formation of outer-sphere complexes can have a directing effect, possibly as a consequence of formation of hydrogen bonds leading to

(44) Elmroth, S. K. C.; Lippard, S. J. *J. Am. Chem. Soc.* **1994**, *116*, 3633−3634.

stereoselective interactions. The remarkable difference between the relative rates for cisplatin (**-GG-** > **-AG-** ≫ **-GA-**) and *cis*-$[Pt(NH_3)_2(OH_2)_2]^{2+}$ (**-GG-** > **-AG-** = **-GA-**) provides support for the suggestion that outer-sphere complex formation plays a determining role.

Alternatively, differences in the stabilities of the transition states that lead to the monofunctional adducts could control the initial binding rates. In this context, it is noteworthy that the G/Cl monofunctional adduct on **-GA-** strongly distorts the duplex structure and, perhaps, indicates that formation of this adduct leads to unfavorable steric interactions that could destabilize the transition state. However, a similar distortion is observed for the G/Cl and G/H_2O adducts, which is not in accord with the rapid formation of the G/H_2O adduct.

Two factors have emerged from this study that address the nonformation of the GpA adduct on duplex DNA. First, monofunctional binding of cisplatin to the GpA sequence is approximately an order of magnitude slower than binding to either GpG or ApG sequences. This factor alone nearly accounts for the nonformation of the GpA adducts, since it leads to the expectation that they would account for less than 4% of the total platination of the DNA. The second factor is the slow closure of the monofunctional adducts. Most studies of cisplatin binding to DNA have been terminated after 24 h, and at this time less than 10% of monofunctional adducts at GpA sequences have closed to form bifunctional adducts. Thus, the two factors together clearly account for the failure to observe these adducts. Reaction of *cis*-$[Pt(NH_3)_2(OH_2)_2]^{2+}$ (**2**) is similar at ApG and GpA sequences, but closure to the bifunctional adduct is again slow for GpA. Thus, the lack of binding at the GpA sequences is not the critical factor in this case. However, after 24 h, bifunctional adducts account for only 15% of the platination; thus, here too, few GpA adducts would be expected.

Possible reasons for the slow rate of closure at GpA sequences have been discussed above, viz., that closure from the 5′ side of the purine-purine side is inherently slower or that repulsion between an NH_3 ligand and the exocyclic NH_2 of adenine slows the closure. Binding to the TpGpGpT sequence shows that closure from the 5′ side is 13-fold slower, confirming the former assertion, at least for this sequence. For TpGpApT, the rate of closure from the 5′ side is similar to that for TpGpGpT sequence. Thus, it appears that the most plausible explanation for the slow closure to give the GpA bifunctional adduct is that initial binding at the G is preferred and then closure from that side is inherently slower.

Acknowledgment. This work was supported by the Australian Research Council (to T.W.H.) and by Griffith University (to S.J.B.-P.). We thank Dr. G. Pierens and Ms. C. Tranter for assistance with NMR experiments.

Supporting Information Available: SCIENTIST models used to determine the rate constants given in Tables 2 and 3, a plot of the time dependence of the platinated **-AG-** duplex aromatic H8 resonance intensities, and an expansion of Figure 6b (6 pages, print/PDF). See any current masthead page for ordering information and Web access instructions.

JA981725U